Elastic Properties and Debye Temperature of Zn Doped $PbTiO_3$ from First Principles Calculation

Hassakorn Wattanasarn[a] & Tosawat Seetawan[a]

[a] Thermoelectrics Research Center, Faculty of Science and Technology, Sakon Nakhon Rajabhat Univesity, 680 Nittayo Road, Mueang District, Sakon Nakhon 47000, Thailand
Published online: 23 May 2014.

PLEASE SCROLL DOWN FOR ARTICLE

Taylor & Francis
Taylor & Francis Group

Elastic Properties and Debye Temperature of Zn Doped PbTiO₃ from First Principles Calculation

HASSAKORN WATTANASARN AND TOSAWAT SEETAWAN*

Thermoelectrics Research Center, Faculty of Science and Technology, Sakon Nakhon Rajabhat Univesity, 680 Nittayo Road, Mueang District, Sakon Nakhon 47000, Thailand

Zn-doped PbTiO₃ has been developed to derive mechanical properties and phase transition. In this paper, a Zn atom 0–16% wt which occupied PbTiO₃ structure was investigated by using first principles density functional theory. The generalized gradient approximation was employed to determine the exchange correlation potential. The findings revealed that Zn-doped PbTiO₃, calculated through Mulliken population analysis, had atomic (both ionic and covalent) bonding. In addition, the elastic constant satisfied the traditional mechanical stability conditions. Bulk modulus, Young's Modulus and Poisson's Ratio were found to increase with increasing Zn contents. Moreover, the result from the calculated longitudinal sound velocity and transverse sound velocity indicated that Debye temperature for Zn-doped PbTiO₃ had more than PbTiO₃. Although the Zn-doped PbTiO₃ has no reported data for comparisons, it is predicted that Zn-doped PbTiO₃ can improve mechanical and dynamics behavior.

Keywords PbTiO₃; Zn; elastic constant; Debye temperature

1. Introduction

Lead titanate (PbTiO₃, PT) ceramics are known as ferroelectric materials [1]. The PT can exhibit excellent dielectric, piezoelectric and pyroelectric properties which are used as electronic sensors and optical electronic devices at high temperatures and high frequencies [2]. PT ceramics are difficult to synthesize through different temperatures and the Curie temperature (T_C), due to a distorted structure of the tetragonal phase at room temperature [3]. The effect of ZnO addition increases the average grain size at lower temperature as a sintering aid. In addition, ZnO reduced the loss of volatile PbO. The ZnO also improved dielectric properties and ferroelectric properties of relaxor ferroelectric ceramics [4]. The properties of PT perovskite were investigated based on Density Functional Theory (DFT). Many researchers have applied DFT to examine perovskite structures. Cohen [5] calculated the phonon frequencies and eigenvectors of PT with DFT. Hosseini [6] calculated the phase diagram of PT by using a first principles approach method. Moreover, the elastic constants (C_{ij}) are important in physics and chemistry. C_{ij} are also determined by the first principles method such as Liu et al.[7] to theoretically study the elastic properties of PbTiO₃.

Theoretically, the ionic radius of Zn is larger than O, then we improved mechanical properties of PT by Zn dopant occupy to O vacancies. In case of, Zn- doped PbTiO₃ (PT/Zn)
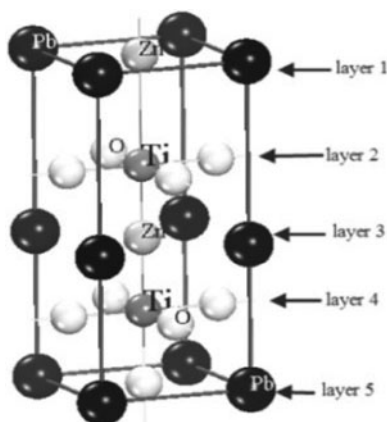
Figure 1. Model unit cell 25-atom in $2 \times 1 \times 1$ of PT. The dark gray, middle gray and white balls represent Pb, Ti and O atoms, respectively. The O vacancies substituted by Zn (light gray ball) and divided into 5 layers.

has not been studied in terms of dynamics behavior and mechanical properties. The paper not only used a Density Functional Theory under first principles study of PT/Zn, but also proved the feasibility of calculating and predicting atomic bond by Mulliken population analysis. In addition, the Zn-doped $PbTiO_3$ confirmed the elastic constants, the longitudinal sound velocity, transverse sound velocity and Debye temperature through the use of GGA for different approximation.

2. Method of Calculation

First principles calculation was performed within the GGA of using the ab initio revised Perdew Burke Ernzerhof [8] for exchange correlation function. The pseudo potentials were adopted to perform with the lowest possible cutoff energy for the plane-wave basis set. The 500 eV energy cut-off was used to smear on perovskite structure surface of PT/Zn. The k-points for the Brillouin zone generated $5 \times 5 \times 2$ for Zn/PT. The energy tolerance was 1.0×10^{-3} eV/atom, the maximum force tolerance was 0.03 eV/Å, and the maximum displacement tolerance was 1×10^{-3} Å. The method of calculation was followed to accomplish in electronic structure by DFT.

3. Results and Discussions

3.1 Structure Properties

PT appears to exist in two different crystal structures, i.e. tetragonal (P4 mm) and cubic (Pm$\bar{3}$m). The positions of O, substituted by Zn atoms in PT tetragonal structure, have been accommodated after synthesizing. These models were simultaneously used to optimize the potential. The supposition was that 1) the $2 \times 1 \times 1$ cell consisted of 25 atoms, which was divided into 5 layers as shown in Figure 1, 2) each cell accommodated a perovskite unit PT where Ti atoms occupied a body center site of each cell, 3) Zn atoms occupied in the cell due to a charge compensation of oxygen vacancies.

The pressure-volume relation dependence of the unit cell for PT was approximated with experimental data by the Birch–Murnaghan equation of state as follows:

$$P = \frac{3}{2}B_0 \left(x^{-7/3} - x^{-5/3} \right) \left[1 + \frac{3}{4} \left(B' - 4 \right) \left(x^{-2/3} - 1 \right) \right] \quad (1)$$

where x (= V/V_0) is the relative unit cell volume, V is the unit cell volume at varying pressure, V_0 is the unit cell volume at zero pressure, and β_0 is the bulk modulus, and $\beta' = (\partial\beta/\partial P)_T$ is first pressure derivative. The Oxygen substituted by Zn atom into PT structure from Zn 0–16% wt contents. In this study, the lattice parameter of PT obtained are a = 3.973 Å, c = 4.223 Å, and the tetragonal distortion parameter (c/a) of 1.063 which were at agreement with the reviewed literature [9]. The c/a of PT/Zn 4% wt was 1.204, decreased to 1.12 at PT/Zn 8% wt and then increased with the increasing PT/Zn 12% wt. This suggested that the PT phases transformed the Zn contents.

3.2 Mulliken Charge and Bond Population

The convergences of a charge distribution were determined by Mulliken population analysis. The charge Q_A was defined as the difference of the electrons in free space. The total electron density (P) was expanded in terms of a set of atomic orbitals P(r), $P(r) = \sum n_i P_i(r)$ when, n_i was account number in the orbital occupation, then $P_i(r) = \sum c_{ai}c_{bi}X_a{}^*X_b$, was replaced by $S_{ab} = X_a{}^*X_b$ which was the overlap matrix. The $D_{ab} = \sum n_i c_{ai}c_{bi}$ was the density matrix, so $P_i(r) = \sum D_{ab}S_{ab}$ when two atoms comprised a and b. The charge Q_A was called the Mulliken charge which was defined as:

$$Q_A = Z_A - \sum P_A(r)\, dr \quad (2)$$

Z_A was the atomic center of positive charge which surrounded an electron cloud.

The bonds population showed positive and negative values which were related to bonding and anti-bonding states, while the values were low (or high) indicating the atomic bond exhibited strong ionic interaction (or covalent bond). As shown in Table 1, $PbTiO_3$ with a valence state of $Pb^{1.09}Ti^{0.95}O_3{}^{-0.77}$, the effective charges of Pb and Ti were estimated at 1.09 and 0.95 respectively. The effective charge on Pb, Ti and only one of Zn in PT/Zn 4% wt and 8% wt was positive whereas the other of Zn in PT/Zn 4–16% wt and O were negative. These implied that the electronegativity of Zn was slightly larger than electronegative of Pb and Ti. The results agreed with the work of Sergio [10]. The bond population results of PT/ZN as shown in Table 1 found that the O-Pb in layer 1, 5, O−Ti in layer 2, 4 and Zn-Pb in layer1, 3, 5 of PT/Zn 4–8% wt were in bonding state, whereas Zn−Ti was bonded in layer 2, and Zn−Pb in layer 5 of PT/Zn 12% wt were in anti-bonding state. It can be concluded that the O−Ti, O−Pb and Zn−Pb bond exhibited covalent bond, whereas Zn−Ti and Zn−Pb bond showed ionic bond behavior.

3.3 Elastic Properties

The thirty six elements of elastic constants (C_{ij}) matrix of tetragonal at high symmetry were reduced to six elements. The elastic behaviors of PT and PT/Zn were described by C_{11}, C_{12}, C_{13}, C_{33}, C_{44} and C_{66} elements. Then C_{ij} was obtained by the use of the stress (σ) and strain (ε) appliance which were in the notation form of $\sigma_{ij} = C_{ij}\varepsilon_j$ and $\varepsilon_i = S_{ij}\sigma_j$, when the S_{ij} ($1/C_{ij}$) was elastic compliance constant.

Table 1
The calculated Mulliken and bonds population for 0–16% PT/Zn compounds

				Muliken charges			
	O	Ti	Zn1	Zn2	Zn3	Zn4	Pb
PT	–0.77	0.95					1.09
4%PT/Zn	–0.78	0.73	0.11				0.9
8%PT/Zn	–0.67	0.68	–0.008	0.28			0.9
12%PT/Zn	–0.69	1.25	–0.59	–0.77	–0.59		0.45
16%PT/Zn	–0.68	1.37	–0.61	–0.76	–0.52	–0.88	0.35
	–0.95[a]	2.18[a]					1.08[a]

					Bonds population			
	Layer1		Layer2		Layer3	Layer4	Layer5	
	O−Pb	Zn−Pb	O−Ti	Zn−Ti	Zn−Pb	O−Ti	O−Pb	Zn−Pb
PT	0.26		0.65			0.88	0.26	
4%PT/Zn	–0.05		1.17		1.18	1.17	0.09	
8%PT/Zn	–0.01		1.43		1.16	1.14		1.12
12%PT/Zn		–0.64	1.29		–1.02	1.29		–1.02
16%PT/Zn		–0.52	1.34	–1.31	0.13	2.38		–1.21

[a]Reference [10].

The elastic constants were calculated by DFT calculations on PT structure, the elastic properties of PT cell can be referred by the theory on Voigt and Reuss approximation. Commonly, the Voigt (subscript V) and Reuss (subscript R) for bulk modulus (B), Young's modulus (E), Poisson ratio (σ), shear modulus (G), and compressibility (β) for PT/Zn according to Voigt and Reuss were as follows [11]

$$B_V = 2C_{11} + 2C_{12} + 4C_{13} + C_{33},$$
$$B_R = \frac{1}{2S_{11} + 2S_{12} + 4S_{13} + S_{33}} \tag{3}$$
$$G_V = \frac{1}{15}\left(2C_{11} - C_{12} - 2C_{13} + C_{33} + 6C_{44} + 3C_{66}\right),$$
$$G_R = \frac{15}{8S_{11} - 4S_{12} - 8S_{13} + 4S_{33} + 6S_{44} + 3S_{66}} \tag{4}$$
$$E_V = \frac{9B_V G_V}{3B_V + G_V}, \quad E_R = \frac{9B_R G_R}{3B_R + G_R}, \quad \beta = \frac{(C_{11} + C_{12})C_{13} - 2C_{13}^2}{C_{11} + C_{12} + 2C_{33} - 4C_{13}}, \tag{5}$$

The B_V, B_R and G_V, G_R according to Hill's empirical were obtained to E, σ and β as the following equation

$$B_H = \frac{B_V + B_R}{2}, \quad G_H = \frac{G_V + G_R}{2}, \quad E_H = \frac{9B_H G_H}{3B_H + G_H}, \quad \sigma = \frac{E_H - 2G_H}{2G_H} \tag{6}$$

The elastic constants which were shown in Table 2 revealed that all the elastic constants exhibited instability with increasing Zn contents. It was also found that, in comparison,

Table 2
The calculated elastic constants, C_{ij} (GPa), bulk modulus B (Gpa), shear modulus G (GPa) and Young's modulus E(GPa) on Voigt and Reuss for PT/Zn wt.%

PT/Zn	C_{11}	C_{33}	C_{44}	C_{12}	C_{13}	C_{66}	B_V	B_R	G_V	G_R	E_V	E_R
PT	156.4	135.4	42.1	46.8	46.3	40.1	81.5	80.9	45.5	44.8	155.2	113.5
4%	163.7	166.8	372.2	71.8	55.1	54.2	118.9	108.3	69.3	36.4	174.3	98.3
8%	150.6	144.5	534.7	84.1	56.2	60.3	135.1	109	48.9	57.2	130.9	146.2
12%	102.3	356.4	34.6	209.6	57.3	27.9	137.7	133.3	4.7	117.4	13.9	272.4
16%	207	348.1	25.2	108.1	86.1	51.1	158.5	152.3	51.9	79	140.5	102.1
PT[a]	235	105	65.1	90	69	98						

[a]Reference [13].

the elastic constants C_{11}, C_{12}, C_{44}, C_{12}, C_{13} and C_{66} were very sensitive to Zn contents. This suggested that Zn atom which substituted O vacancy had an effect to phase transform. If this structure was stable, it should satisfy the mechanical stability under the isotropic pressure which were relatively judged in of six element of tetragonal structure as seen in the following equation [12], $(C_{11}-C_{;12}) > 0$, $(C_{11} + C_{33}-2C_{13}) > 0$, $(2C_{11} + C_{33} + 2C_{12} + 4C_{13}) > 0$, $C_{11} > 0$, $C_{33} > 0$, $C_{44} > 0$ and $C_{66} > 0$. While the B_V, B_R, G_V, G_R, E_V and E_R of Zn doped PT changes from 0–16% were listed in Table 2, it increased with increasing Zn contents. However, the PT/Zn 12% wt has G_V, G_R, E_V and E_R different from the Zn other contents, due to Zn atom site in PT structure.

The elastic moduli were related to the hardness and strength of materials structure. The elastic moduli of PT/Zn, as shown in Table 3, revealed that the results were lower than reference [13, 14], due to the supposition of the PT/Zn structure which has a larger unit

Table 3
The PT/Zn 4–16% wt relative with Hill bulk modulus (B_H), Hill Young modulus (E_H), Hill shear modulus (G_H), Poisson ratio (σ), compressibility ($\beta \times 10^{-3}$ GPa^{-1}), B_H/G_H ratio, longitudinal, transverse, average sound velocity (v_τ, v_l, v_m m/s), and Debye temperatures (θ_D)

	PT	4%	8%	12%	16%	PT
B_H	81.19	113.62	122.03	135.53	155.44	104[a]
G_H	45.2	52.93	53.09	61.06	65.48	61.5[a]
E_H	114.38	137.44	139.1	159.27	172.26	134[b]
σ	0.76	0.798	0.81	0.804	0.815	0.3[b]
β	12.36	9.23	9.17	77.5	5.6	
B_H/G_H	1.79	2.15	2.98	2.22	2.37	
v_t	22347.9	2486.6	2608.9	2744.6	2920.2	2771.4[cc]
v_l	4153.6	4638.7	4971.9	5229.9	5622.45	4789[c]
v_m	2611.3	2776.9	2917.8	3100.8	3268.2	3076.1[c]
θ_D	335.1	340.2	347	370.8	386.6	393.8[c],337[d]

[a]Reference [14], [b]Reference [12], [c]Reference [18] and [d]Reference [19] experiment.

cell of PT. The B_H, G_H, and E_H increases with the increasing of Zn contents. It implied that the Zn atoms can improve the PT stiffness; only the B values decreased with increasing Zn contents, which were behavior of materials structure. The Pugh's criterion, [15] was able to predict the B_H/G_H ratio; if the value was larger than 1.75, the material will be ductile. The calculation of the B_H/G_H ratios range was at 1.79 to 2.37 for PT/Zn 0–16% wt, which indicated that PT/Zn had a ductility which increased with increasing Zn contents. In addition, the σ was associated with covalent bond, if the value was smaller than 0.1, whereas ionic bond had a value larger than 0.25 [17], the Poisson ratio was at 0.76 to 0.815 for PT/Zn. 0–16% wt. The calculation results showed that the atomic bond of PT/Zn had more ionic bond than covalent bond.

3.4 Calculation of Debye Temperature

Commonly, the morphotropic phase boundary should be correlated with Debye temperatures of materials. The method to determine the Debye temperature (θ_D) was estimated from the average sound velocity (v_m) as in the following equation [17]

$$\theta_D = \frac{h}{k_B} \left[\frac{3}{4\pi V_a} \right]^{1/3} v_m \tag{7}$$

when h was the Plank's constant, k_B was the Boltzmann's constant and V_a was the atomic volume. The average sound velocity in the material was given by [17]

$$v_t = \left(\frac{G_H}{\rho} \right)^{1/2}, \; v_l = \left(\frac{3B_H + 4G_H}{3\rho} \right)^{1/2}, \; v_m = \left[\frac{1}{3} \left(\frac{2}{v_t^3} + \frac{1}{v_l^3} \right) \right]^{-1/3}, \tag{8}$$

v_t and v_l were the transverse and longitudinal sound velocity which were obtained from the Hill's shear modulus G_H and bulk modulus β_H and ρ were the density of the composites.

The calculated sound velocity and Debye temperature as well as the density for PT/Zn % wt were given in Table 3. The results from the calculation of the transverse and longitudinal sound velocity and Debye temperature at 335 K, increases with the increasing of Zn contents were in accordance with current literature [18, 19], which suggests an increasing Debye temperature, since Zn content would affected to T_C of PT.

4. Conclusions

In this work, the lattice constants, Mulliken population, elastic constants, and Debye temperature of tetragonal PT/Zn 0–16% wt have been calculated for the first time by using density functional theory. The Zn atoms had an effect on the lattice constants of PT cell, while tetragonal distortion created more experimental values. The Mulliken population showed the atomic bond between PT and Zn atoms which were composed of ionic bond and covalent bond. It was found that the tetragonal PT/Zn had elastic constants satisfying the mechanical stability conditions. By calculation with bulk modulus, shear modulus, Young's modulus and Poisson ratio of the tetragonal, we showed increasing Zn contents and PT/Zn demonstrating ductile properties. Poisson ratios revealed that the PT/Zn had more ionic bond than covalent bond. The Debye temperature of PT was calculated at 335 K and increased with increasing Zn contents. Unfortunately, there were no literature data for PT/Zn on these properties. These results may be useful for ferroelectric materials.

References

1. G. Shirane, R. Pepinsky, and B. C. Fraze, X-ray and neutron diffraction study of ferroelectric $PbTiO_3$. *Acta Crystallogr.* **9**, 131 (1956).

2. A. J. Moulson, and J. M. Herbert, *Electroceramics,* 2nd ed., Wiley: Chichester; (2003).

3. E. C. Paris, M. F. C. Gurgel, T. M. Boschi, M. R. Joya, P. S. Pizani, A. G. Souza, E. R. Leite J. A. Varela, and E. Longo, Investigation on the structural properties in Er-doped $PbTiO_3$ compounds: A correlation between experimental and theoretical results. *J. Alloys and Compound.* **462**, 159. (2008).

4. M. Bonyani, A. Mirzaee, A. Barzegar, and M. R. Saeri, Effect of nano ZnO addition on microstructure and dielectric properties of Pb $(Zn_{1/3}Nb_{2/3})$ O_3 $PbTiO_3$–$BaTiO_3$ (PZN–PT–BT) relaxor ferroelectric. *Micro & Nano Letters.* **7**, 762–765. (2012).

5. R. E. Cohen, and H. Krakauer, Lattice dynamics and origin of ferroelectricity in $BaTiO_3$: Lanearized augmented plane wave total energy calculations. *Phys. Rev. B.* **42**, 6416 (1990).

6. S. M. Hosseini, T. Movlarooy, and A. Kompany, First-principles study of the optical properties of the cohesive energy and the electronic properties of $PbTiO_3$. *Physica. B.* **391**, 316 (2007).

7. Y. Liu, G. Xu, C. Song, Z. Ren, G. Han, and Y. Zheng, First-principlesstudy of elastic properties in perovskite $PbTiO_3$: Materials Scienceand Engineering A: *Structural Materials, Properties, Microstructure and Processing*. **472**, 269–272 (2008).

8. B. Hammer, L. B. Hansen, and J. K. Norskov, Improved adsorption energetics within densityfunctional theory using revised Perdew-Burke-Ernzerhof functionals. *Phys. Rev. B.* **59**, 7413 (1999).

9. R. Wongmaneerung, S. Choopanb, R. Yimnirun, and S. Ananta, Dielectric properties of $PbTiO_3$/ZnO ceramic nanocomposites obtained by solid-state reaction method, *J. Alloys and Compound.* **509**, 3547–3552 (2011).

10. S. Lazaro, E. Longo, J. R. Sambrano, and A. Beltran, Structural and electronic properties of $PbTiO_3$ slabs. *Surface Science.* **552**, 149–159 (2004).

11. D. E. Kim, S. L. Shang, and Z. K. Liu, Phase separation in metallic and mechanical properties of Fe-based ultrafine eutectic composites. *Intermetallics.* **18**, 1164e1165 (2010).

12. X. R. Chen, X. F. Li, L. C. Cai, and J. Zhu, Pressure induced phase transition in ZnS. *Solid State Commun.* **139**, 246 (2006).

13. N. Choudhury, E. J. Walter, A. I. Kolesnikov, and C. K. Loong, Large phonon band gap in $SrTiO_3$ and the vibrational signatures of ferroelectricity in $ATiO_3$ perovskites: First-principles lattice dynamics and inelastic neutron scattering. *Phys. Rev. B.* **77**, 134111 (2008).

14. L. Jianping, L. Yang, and X. Wei, Lattice, elastic properties and Debye temperatures of $ATiO_3$ (A = Ba, Ca, Pb, Sr) from first-principles. *J. Alloys and Compounds.* **549**, 336 (2013).

15. S. F. Pugh, XCII. Relations between the elastic moduli and the plastic properties of polycrystalline pure metals. *Philosophical Magazine.* **45**, 823–843 (1954).

16. I. R. Shein, and A. I. Ivanovskii, Elastic properties of quaternary oxypnictides LaOFeAs and LaOFeP as basic phases for new 26–52 K superconducting materials from first principles. *Scr. Mater.* **59**, 1099 (2008).

17. O. L. Anderson, A simplified method for calculating the Debye temperature from elastic constants. *J. Phys. Chem. Solids.* **24**, 909 (1963).

18. W. N. Lawless, N. Terutaro, M. Takashige, and S. L. Swartz, Specific Heat of Amorphous and Crystalline $PbTiO_3$ at Low Temperatures. *Phys. Soc. Jpn.* **52**, 207–214 (1983).

19. J. Long, L. Yang, and X. Wei, Lattice, elastic properties and Debye temperatures of $ATiO_3$ (A = Ba, Ca, Pb, Sr) from first-principles. *J. Alloys and Compounds.* **549**, 336–340 (2013).